CRR9/CLPTM1L Regulates Cell Survival Signaling and is Required for Ras Transformation and Lung Tumorigenesis

Michael A. James, **Haris G. Vikis**, **Everett Tate**, **Amy L. Rymaszewski**, and **Ming You**

MCW Cancer Center, Department of Pharmacology and Toxicology, Medical College of Wisconsin, 8701 Watertown Plank Rd., Milwaukee, Wisconsin 53226

Abstract

The transmembrane protein CLPTM1L is overexpressed in non-small cell lung cancer (NSCLC) where it protects tumor cells from genotoxic apoptosis. Here we show that RNAi-mediated blockade of CLPTM1L inhibits K-Ras-induced lung tumorigenesis. CLPTM1L expression was required in vitro for morphological transformation by H-RasV12 or K-RasV12, anchorage independent growth and survival of anoikis of lung tumor cells. Mechanistic investigations indicated that CLPTM1L interacts with PI3K and is essential for Ras-induced AKT phosphorylation. Further, that the anti-apoptotic protein Bcl-xL is regulated by CLPTM1L independently of AKT activation. Constitutive activation of AKT or Bcl-xL rescued the transformed phenotype in CLPTM1L-depleted cells. The CLPTM1L gene lies within a cancer susceptibility locus at chromosome 5p15.33 defined by genome-wide association studies. The risk genotype at the CLPTM1L locus was associated with high expression of CLPTM1L in normal lung tissue, suggesting that cis-regulation of CLPTM1L may contribute to lung cancer risk. Taken together, our results establish a pro-tumorigenic role for CLPTM1L that is critical for Ras-driven lung cancers, with potential implications for therapy and chemosensitization.

Introduction

Cisplatin Resistance Related Protein-9 (CRR9), otherwise known as Cleft-Lip and Palate Transmembrane Protein-1-Like (CLPTM1L) has been found to be highly expressed in cisplatin resistant ovarian tumor cell lines (1). We recently found CLPTM1L to be overexpressed and associated with resistance to genotoxic apoptosis in human lung tumors and lung tumor cell lines (2), a finding subsequently confirmed by others (3). Our previous results demonstrated that CLPTM1L conferred resistance to apoptosis through up-regulation of Bcl-xL (2), an anti-apoptotic Bcl-2 family member (4). Very little else is known about the

Correspondence: Dr. Michael James, MCW Cancer Center, Department of Pharmacology and Toxicology, Medical College of Wisconsin, 8701 Watertown Plank Rd. Milwaukee, Wisconsin 53226. Dr. Ming You, MCW Cancer Center, Department of Pharmacology and Toxicology, Medical College of Wisconsin, 8701 Watertown Plank Rd., Milwaukee, Wisconsin 53226. mjames@mcw.edu; myou@mcw.edu.

function of CLPTM1L, although it is suggested by affinity capture – mass spectrometry to interact with PI3-Kinase (5). The PI3K/AKT pathway is activated by oncogenes including Ras, and provides proliferative and survival signals to tumor cells (6). AKT is also known to activate NFκB (6), which can in turn directly regulate Bcl-xL (7), making this signaling cascade of interest in regard to CLPTM1L-mediated resistance to apoptosis.

The CLPTM1L gene resides within a locus at chromosome 5p15.33 (*TERT-CLPTM1L*) shown by multiple genome wide association studies (GWAS) to be associated with lung and other cancers such as cervical, pancreatic, bladder, glioma, prostate, basal cell carcinoma and melanoma (8–18). A *CLPTM1L* haplotype has been found to confer glioma risk (16). Chromosome 5p is commonly duplicated in cervical cancer cell lines, however, of the genes within the cancer associated 5p15.33 region, only CLPTM1L is overexpressed (19). Our previous studies demonstrated that CLPTM1L is overexpressed in lung adenocarcinoma (2). Furthermore, copy number gain of the 5p15.33 region has been found to be the most common genetic event in early stage NSCLC tumors (20). Independent genetic association observations within both *TERT* and *CLPTM1L* genes suggests that each of these genes may constitute separate association loci and that one or both may be involved in lung cancer susceptibility (11). Evidence, including a recent meta analysis, suggests that the *TERT* locus (rs2736100) is specific to adenocarcinoma histology, while the *CLPTM1L* locus (rs401681) is associated with all lung tumor histologies including squamous cell carcinoma, adenocarcinoma, small cell carcinoma and large cell carcinoma (15, 21).

Here we demonstrate that CLPTM1L is required for Ras transformation of mouse fibroblasts. In addition, we show that CLPTM1L is required for lung tumorigenesis in a conditional K-Ras^{G12D} transgenic mouse model. Furthermore, this study demonstrates that this mouse model can be successfully used to evaluate post-GWAS candidate modifiers of lung tumorigenesis. We also show that CLPTM1L protects lung tumor cells from anoikis. Our data demonstrates that CLPTM1L is necessary for the sustained Ras induced accumulation of phosphorylated AKT and Bcl-xL, independently. Regulation of AKT activity may be due to an interaction with PI3K catalytic subunits, which we have demonstrated by co-immunoprecipitation. A robust inhibition of Ras driven *in vitro* transformation and *in vivo* tumorigenesis upon depletion of CLPTM1L establishes this protein as a pro-tumorigenic factor required for oncogenesis by K-Ras. This inhibition of transformation was dependent on inhibition of both AKT phosphorylation and Bcl-xL expression. Our studies strongly implicate protection from apoptosis and regulation of apoptotic effectors as mechanisms for the pro-tumorigenic function of CLPTM1L. Furthermore, association of the risk genotype at 5p with high expression of CLPTM1L suggests that cis-regulation of this gene may contribute to lung cancer risk.

Materials and Methods

Cell Culture, Knockdown and Overexpression

Human lung adenocarcinoma cell ines (A549 and H838) and Spon 8 mouse lung tumor cell lines were cultured in RPMI1640 plus 2% FBS (Invitrogen, Carlsbad, CA). Beas-2B were cultured in LHC-8 media plus epinephrine (Invitrogen, Carlsbad, CA), and NIH3T3 were cultured in DMEM media with 10% FBS (Invitrogen, Carlsbad, CA). Cells were transduced

with lentiviral short-hairpin RNA (shRNA) vectors based on the pLKO.1 vector and designed to specifically target human CLPTM1L transcript (Sigma, St. Louis). Empty vector, scrambled shRNA vector or vectors targeting CLPTM1L transcript were first packaged in 293T cells (Orbigen, San Diego, CA) by transfection with helper plasmids using Lipofectamine LTX (Invitrogen, Carlsbad, CA) and then transduced into A549 cells with 8 μg/ml Polybrene (Sigma, St. Louis, MO). Media was replaced 24 hours after transduction, and cells were split 1:4 48 hours after transduction. At 72 hours post transduction, cells harboring lentiviral constructs were selected with 1 μg/ml puromycin for 2–4 days, until mock infected cells were dead. Surviving cells were pooled. Mouse cells were transduced and selected similarly with shRNA constructs designed to target mouse CLPTM1L transcript. NIH3T3 cells were transfected using Lipofectamine LTX with pBABE:empty vector or pBABE:H-RasV12, pLKO.1:vector or pLKO.1:shCLP. shCLP used in NIH3T3 and mouse studies is identical to sh2 in figure S4. For myrAKT studies, the above described stable cell lines were transfected with pBABE:myrAKT or empty vector and assayed after 48 hours. For Bcl-xL studies the above described stable cells were transfected with pSFFV:Bcl-xL plasmid (# 8749 Addgene) or empty vector and selected with G418 until mock transfected cells were dead. Cells were plated at 200,000 cells per well on 6 well tissue culture dishes and assayed after 48 hours. Authenticated A549, H838, Beas-2B and NIH3T3 cells were obtained from ATCC within 6 months of experiments. Spon 8 cells were developed from spontaneous and metastatic lung tumors from A/J mice by our laboratory when housed at The Ohio State University in 1996 and are characterized in (22) and (23). These cells are periodically authenticated based on the molecular profile described in therein, which was performed within 3 months of their use in experiments.

RT-Quantitative Real-Time PCR

Patient matched tumor and tumor-adjacent normal RNA samples were obtained from the Tissue Procurement Core at Washington University in St. Louis under protocol approved by the Institutional Review Board at Washington University in St. Louis School of Medicine, Human Research Protection Office. Written consent was obtained from all patients participating in this tissue bank. RNA was isolated from cell lines using Tri-zol reagent and protocols (Invitrogen, Carlsbad, CA). Quantitative real-time PCR (qPCR) was conducted using the method as described previously (Chaparro, Wen et al. 2005). Briefly, one microgram of total RNA per sample was converted to cDNA using the SuperScript First-Strand Synthesis system for RT-PCR (Invitrogen, Carlsbad, CA). Quantitative RT-PCR assay was done using the SYBR Green PCR Master Mix (Applied Biosystems, Foster City, CA). One microliter of cDNA was added to a 25 μL total volume reaction mixture containing water, SYBR Green PCR Master Mix, and primers. Each real-time assay was done in duplicate on a BioRad MyIQ machine. Data were collected and analyzed with Stratagene Mx3000 software. The *β-actin* gene (Actb) was used as an internal control to compute the relative expression level (C_T) for each sample. Primer set efficiency and linearity was calculated, and normalization was performed in accordance with MIQE guidelines. The fold change of gene expression in tumor tissues as compared to the paired normal tissues was calculated as 2^d, where d = $C_{T\ normal} - C_{T\ tumor}$. P-values were determined using a two-tailed Student's *t*-Test.

Western Blotting

Cells were lysed with 100 µl of 1X NP40 lysis buffer containing proteinase inhibitors, sheared 10 times with a 28 gauge needle, spun at $16,000 \times g$ for 30 minutes, normalized by protein concentration as determined by the Bradford method, and the supernatant boiled for 5 min. 20 µl of normalized lysate was resolved by SDS-PAGE and immunoblotting analyzed with indicated antibodies. The following antibodies were used: rabbit anti-CLPTM1L (Novus Biologicals, Littleton, CO), mouse anti-Actin (Santa Cruz Biotechnology, Santa Cruz, CA), mouse anti-Bcl2 clone 124 (Dako, Carpinteria, CA), rabbit anti-Bax #2774 (Cell Signaling, Boston, MA), mouse anti-p53 (Ab-1) (Oncogene, San Diego, CA), Bcl-xL – rabbit Bcl2L1 (AbCam, Cambridge, MA), rabbit anti-H-Ras (Novus Biologicals, Littleton, CO), mouse anti-K-Ras (BD Transduction Labs, Franklin, NJ), anti-AKT (Cell Signaling, Boston, MA), anti-pAKT (Thr308)(Cell Signaling, Boston, MA), rabbit anti-PIK3C3 (Cell Signaling, Boston, MA), rabbit anti-BAD (AbCam, Cambridge, MA). Quantitation of Western analyses of three independent cultures was done using Image J software (24).

Co-Immunoprecipitation

Antibodies for bait proteins (PIK3C3, PIK3CA, CLPTM1L and Actin, described above) were immobilized covalently using amino-link columns from Pierce Co-Immunoprecipitation Kit, (Peirce, Thermo Scientific, Rockford, IL) according to manufacturer's protocol. Lysates were obtained, cleared on agarose resin and immunoprecipitated according to the protocol. Western blotting for PI3K or CLPTM1L was performed on IP eluates as described above. Immobilized Actin antibody was used as irrelevant bait. IP column flow through with no bait antibody was run as an input control.

shRNA/K-Ras^{LSL-G12D/+} Mouse Model of Lung Tumorigeneis

Mouse experiments were conducted as described by M. DuPage, A. L. Dooley, T. Jacks, *Nat Protoc* 4, 1064 (2009) (25), with the following modifications. pLKO.1 empty shRNA vector was obtained from Open Biosystems (Foster City, CA). Short hairpin inserts were designed to specifically target transcripts. Oligos were ordered from IDT (Coralville, IA). Complimentary oligos were heated to 95C, cooled to room temperature overnight and ligated into digested pLKO.1. Vectors were modified by replacing the PGK promoter and puromycin resistance orf with the CMV promoter driving expression of CRE-GFP. CMV promoter was sub-cloned from pLenti CMV GFP Puro plasmid #17448 (Addgene) and CRE-GFP was sub-cloned from pCAG:CRE-GFP plasmid # 13776 (Addgene). Virus was packaged in 293T cells and functionally titered by infecting 3TZ cells (LSL-LacZ), which express LacZ upon Cre recombinase activation. Mice were anesthetized with 200µL Avertin (40µg/ml). 10^4 or 10^3 active virus particles in 50µl of phosphate buffered saline was delivered via intratracheal intubation using a 22 gauge IV catheter under general anesthesia to 10 transgenic mice per group (LSL-K-RasG12D (Mouse Models of Human Cancers Consortium (MMHCC) Strain 01XJ6, Jackson Laboratory #008179 (B6), #008180 (129)). After 24 weeks, mice were anesthetized and euthanized by cervical dislocation. The thoracic cavity was surgically opened to expose the lungs. The trachea was cannulated with a 22G catheter and lungs were inflated with Tellyesniczky's solution (70% ethanol, 2% formaldehyde, and 5% glacial acetic acid) at 25 cm of pressure by gravity. Lungs were fixed

overnight and the solution was exchanged to 70% ethanol the next day. Lungs were photographed, lobes were separated and cleaned. Tumors were counted and measured with digital calipers. A cutoff for visible tumors of 0.2mm diameter was used. Tumor volume was determined by the following formula: $A = 4/3 \pi r^3$. P-values were determined using a two-tailed Student's t-Test.

Transformation assays

NIH3T3 cells acquired within the last 6 months from ATCC were cultured in DMEM 10% FBS to 80% confluence before co-transfecting with the indicated expression and shRNA vectors using Lipofectamine LTX (Invitrogen, Carlsbad, CA). Cells were split, allowed to attach and placed on puromycin selection for 3 days or until mock transfected cells were dead. Cells were plated at the indicated densities and fed as needed. For whole plate staining, cells were fixed in cold methanol and stained with crystal violet. For anchorage independent growth, cells were suspended in 0.4% agarose in complete growth media and plated over 0.8% bottom agar at 10,000 cells per well (H-Ras) or 20,000 cells per well (K-Ras) of a six-well tissue culture dish in triplicate. Cells were fed twice a week over 4 weeks in culture, and colonies were stained using cell staining reagent and protocol from Millipore's Cell Transformation Detection Assay. Images of wells were captured and analyzed by Image J software to count colonies. P-values were determined using a two-tailed Student's t-Test.

Anoikis assay

2×10^5 cells were plated on either conventional treated 6-well tissue culture plates (TPP, Trasadingen, Switzerland) or on poly-hema coated, non-adherent 6-well tissue culture plates (Sciencell, Carlsbad, CA) with 1μM CellPlayer green fluorescent caspase3 substrate (Essen Bioscience, Ann Arbor, MI) and analyzed on an Incucyte FLR live cell imager (Essen Bioscience, Ann Arbor, MI) over 44 hours in culture for caspase positive cells.

Nude mouse xenograft assay

Tumor cells stably expressing shRNA vectors as described above were cultured, counted and resuspended in sterile PBS at a concentration of 2.5×10^6 cells/mL. A volume of 200 μL (5 $\times 10^5$ cells respectively) were injected subcutaneously into the right (vector) or left (shRNA) flank of athymic nude mice at an age of 8 weeks. The health of these mice was monitored 3 times weekly and tumor sizes were measured periodically until sacrifice at 4 weeks post injection. Tumors were removed and weighed. Protein was collected from approximately 30mg of tumor tissue by homogenization with a Tisuelyser LT and 5mm steel beads (Qiagen, Venlo, Netherlands) in RIPA buffer (Sigma, St. Louis) with protease and phosphatase inhibitors. P-values were determined by two-tailed Student's t-test.

Results

High Expression of CLPTM1L in Lung Tissue Correlates with Disease Associated Genotype

In 30 lung adenocarcinomas, CLPTM1L expression averaged 2.8 fold greater in tumor tissue than in matched normal lung tissue (p<0.005) (Figure 1A). Of these patients, 25 (83%)

overexpressed CLPTM1L over adjacent normal tissue (19 (63%) by 1.5 fold), with a maximum of 8.7 fold. Publicly available data analyzed and visualized using Oncomine™ from Compendia Bioscience in Ann Arbor, MI, similarly shows highly significant up-regulation of expression of CLPTM1L in lung squamous cell carcinoma ($p < 5 \times 10^{-33}$) and lung adenocarcinoma ($p < 5 \times 10^{-14}$) compared to normal lung tissue (Figure S1), as well as in many other cancer types (data not shown). With the knowledge that CLPTM1L is commonly overexpressed in lung adenocarcinoma (Figure 1A) (2), and that genetic polymorphisms within CLPTM1L are associated with risk of developing lung cancer (8, 9, 11, 15), we investigated whether expression in tumor adjacent normal lung tissue correlated with the disease associated polymorphisms within the gene. We therefore genotyped the rs31489 lung cancer variant and evaluated expression of CLPTM1L transcripts in tumor adjacent normal lung tissues of 32 adenocarcinoma patients. This variant is one of the most significant risk variants in multiple GWAS studies (9, 17), and is in strong linkage disequilibrium (LD) with rs402710 and rs401681 lung cancer variants. High expression of CLPTM1L in tumor adjacent normal tissues of 32 lung adenocarcinoma patients strongly correlated with the risk genotype at rs31489 (C) ($p < 0.0005$) (Figure 1B and S2). In agreement with our findings, a 2012 study by Grundberg et al. (26) showed an association of CLPTM1L expression with the same CLPTM1L SNPs in adipose tissue of 856 healthy female twins (Figure S3). The SNPs identified in this study are in perfect concordance with lung cancer associated SNPs.

CLPTM1L Interacts with PI3K and is Required for Ras-Induced AKT Activation and Bcl-xL Accumulation

Given evidence that CLPTM1L may interact with catalytic subunits of PI3K (PIK3C3 and PIK3Calpha) (5) and regulates survival of tumor cells (2), we investigated the effect of CLPTM1L on AKT phosphorylation and its interaction with PI3K. Co-immunoprecipitation was performed on NIH3T3 cell lysates using PI3K, CLPTM1L or beta-actin control antibody immobilized covalently on a resin column. Immunoprecipitates and control lysate were immunoblotted for PI3K or CLPTM1L. CLPTM1L co-precipitated with PI3K class III and class I alpha catalytic subunits, but not with Actin control antibody, both when used as bait and prey (Figure 2A).

Survival signaling by PI3K in tumor cells is often mediated by phosphorylation of AKT (6). To investigate the effect of CLPTM1L on AKT signaling, and with the goal of performing transformation and anchorage independence assays (discussed below), oncogenic K-Ras^{V12} was co-expressed in NIH3T3 mouse fibroblasts along with shRNA targeting CLPTM1L. A panel of lentiviral shRNA constructs was evaluated for CLPTM1L knockdown efficiency. Multiple shRNA constructs with CLPTM1L knockdown efficacy conferred a decrease in Bcl-xL expression as well as sensitivity to cisplatin killing, with both phenotypes correlating with the level of CLPTM1L depletion (Figure S4A). Phenotypic results with multiple shRNA constructs targeting CLPTM1L minimize the possibility of any off target effects. The sh2 construct demonstrated the best knockdown efficiency, and was subsequently used for knockdown studies in mouse cells (hereafter referred to as shCLP). Western blotting of lysates from NIH3T3 cells with K-Ras^{V12} and/or shCLP demonstrated a decrease in Bcl-xL expression with loss of CLPTM1L (Figure 2B). This data is consistent with our previous observations in mouse and human lung tumor cells, in which both a decrease in Bcl-xL

expression and sensitivity to genotoxic apoptosis accompanied CLPTM1L depletion (2) and (Figure S4). Expression of K-Ras^{V12} in NIH3T3 cells increased levels of both Bcl-xL and phosphorylated (T308) AKT (Figure 2B). However, when CLPTM1L was stably depleted with shRNA in K-Ras^{V12} expressing cells, the elevation of both Bcl-xL and phospho-AKT was ablated.

CLPTM1L is Required for Ras Induced Oncogenic Transformation and Anchorage Independent Growth

To determine if CLPTM1L is required for oncogenic transformation by Ras, we co-transfected NIH3T3 mouse fibroblasts with expression vectors for H-Ras^{V12} or K-Ras ^{V12}, and shRNA targeting CLPTM1L (shCLP). Stable transfection of either H-Ras^{V12} or K-Ras^{V12} induced a transformed morphology (Figure 3A). The transformed cells grew in crossing spindle patterns with foci growing into dense spheroids that sometimes detached and became free-floating, as has been previously described in oncogenic K-Ras expressing NIH3T3 cells (27). However, upon stable co-transfection of shCLP with either H-Ras^{V12} or K-Ras^{V12}, a nearly complete reversion of the phenotype occurred, and no spheroids were observed. Cells with Ras^{V12}/shCLP displayed altered morphology compared to vector controls, but they did not form dense foci or grow in anchorage-independent spheroids. Cells with shCLP alone did not demonstrate morphological changes compared to vector controls. Exogenous overexpression of Ras^{V12} and knockdown of CLPTM1L was confirmed by Western blotting. To further determine the effect of CLPTM1L depletion on the ability of Ras transformed NIH3T3 cells to grow in an anchorage independent manner, soft agar tissue culture was employed. Expression of H-Ras^{V12} induced anchorage independence, forming an average of 18 colonies per well in soft agar (Figure 3B), whereas H-Ras^{V12} expressing cells with CLPTM1L depletion formed an average of only one colony per well in soft agar, representing a 94% inhibition of colony formation (p<0.05). Similarly, K-Ras^{V12} transfection transformed NIH3T3 cells. With twice as many cells plated as were plated for HRas^{V12} soft agar assays, KRas^{V12} transformed NIH3T3 cells formed 56 colonies per well, which was inhibited by 47% upon CLPTM1L depletion (p<0.05), demonstrating a requirement for CLPTM1L for oncogenic Ras induced anchorage independent growth.

AKT Activity and Bcl-xL Expression are Independently Sufficient to Reconstitute Ras Oncogenic Transformation in CLPTM1L Depleted Cells

To investigate the role of AKT phosphorylation and Bcl-xL expression in the CLPTM1L mediated effects on Ras transformation, we expressed constitutively active myristoylated AKT (myrAKT), Bcl-xL or the corresponding empty vectors in our stable NIH3T3 cell lines expressing KRas^{V12} and shCLP. Expression of myrAKT rescued the transformed phenotype in NIH3T3 cells with KRas^{V12} expression and CLPTM1L depletion (Figure 4A). Reconstitution of either AKT signaling or Bcl-xL resulted in formation of spheroids and macroscopically visible foci. Similarly, re-expression of exogenous Bcl-xL rescued Ras transformation, indicating that either maintenance of AKT phosphorylation or Bcl-xL regulation is sufficient for the effect of CLPTM1L on KRas transformation. Expression of phosphorylated myrAKT and Bcl-xL were confirmed by Western blotting (Figure 4B). Expression of myrAKT did not alter Bcl-xL expression or its regulation by CLPTM1L,

indicating that Bcl-xL is regulated by a separate mechanism and that each is independently sufficient for Ras transformation in CLPTM1L depleted cells.

CLPTM1L Protects Human Lung Tumor Cells from Anoikis and is Required for Tumorigenesis

To determine if CLPTM1L is similarly necessary in lung tumor cells for survival of anchorage detachment, assays for anoikis were employed. A549 cells with stable CLPTM1L depletion using two independent shRNA vectors (shCLP or shCLP*) or scrambled shRNA control were plated in triplicate on poly-HEMA coated plates to prevent attachment, as well as conventional coated tissue culture plates. Non-adherent cells transfected with control vector grew in clusters of refractile cells (Figure 5A). Non-adherent cells with CLPTM1L depletion grew in clusters that generally appeared flat and dull. Apoptotic cell numbers were monitored in real time using a fluorescent caspase 3 substrate and live cell imaging system over 44 hours in culture. Apoptosis was induced to a significant degree on a non-adherent surface only when CLPTM1L was depleted using either shRNA vector, demonstrating that CLPTM1L is critical for protection of lung tumor cells from anoikis ($p<0.05$) (Figure 5B). Depletion of CLPTM1L in A549 cells with shCLP and shCLP* was confirmed by Western blot (Figure 5C). Similar robust induction of anoikis with CLPTM1L depletion using shCLP* was observed in H838 human lung adenocarcinoma cells (K-H- and N-Ras wild-type/p53^{E62*}), demonstrating that the critical survival role of CLPTM1L is not limited to Ras mutant or p53 competent tumor cells ($p<5\times10^{-6}$) (Figure 5D and 5E). H838 cells with scrambled vector grew as mostly separated cells in poly-HEMA coated wells, while CLPTM1L depleted H838 cells grew in aggregates (Figure 5D). Depletion of CLPTM1L was confirmed by Western blot (Figure 5F). We conducted xenograft experiments in athymic nude mice to determine if CLPTM1L depletion affected the ability of A549 human lung tumor cells to form tumors. 5×10^5 A549 cells with either CLPTM1L depletion or with scrambled shRNA control were injected subcutaneously into the left or right flank, respectively. Over four weeks, A549 cells with CLPTM1L depletion formed significantly smaller tumors (average weight = 72 mg), compared to control tumors (average weight = 254 mg) ($p<0.00005$) (Figure 6A). Depletion of CLPTM1L protein in tumors was confirmed by Western blot (Figure 6B).

CLPTM1L is Required for Lung Tumorigenesis in a shRNA/K-Ras$^{LSL-G12D/+}$ Mouse Model

A recently developed model of lung cancer in *K-Ras*$^{LSL-G12D/+}$ transgenic mice utilizes intratracheal delivery of lentivirus expressing CRE recombinase to activate oncogenic K-Ras expression. This model also permits simultaneous expression of short hairpin RNAs targeting a gene of interest, via the same viral vector (25) and is thus particularly well suited to the investigation of potential modifiers of lung tumorigenesis. We utilized this model to induce oncogenic K-Ras driven lung tumors in a cellular environment that is depleted of CLPTM1L (Figure 7A). We also evaluated depletion of TERT in this model to agnostically approach 5p susceptibility candidates. Several lentiviral shRNA vectors targeting TERT or CLPTM1L were designed and evaluated for knockdown of their target transcripts in the Spon8 mouse lung tumor cell cells. Vectors shCLP2 and shTERT1 accomplished knockdown at the transcript level of 80% and 50% for CLPTM1L and TERT, respectively (Figure 7B and Figure S5), and were subsequently used in the mouse model studies. Virus

particles were packaged, and titered by infection of 3TZ cells for quantification of the number of CRE dependent LacZ-inducing particles per milliliter. Mice were subsequently infected with 10^4 functional particles (high dose group) or 10^3 particles (low dose group) by intratracheal intubation. After 24 weeks, lungs were harvested and lung tumors were counted and sized for the high dose group. Most tumors were 1mm in diameter with a few larger tumors. Mice in the high dose group with a non-specific scrambled shRNA had an average of 115 tumors per mouse with an average tumor load of 13.2 mm^3 (Figure 7C and 7E), while mice with CLPTM1L depletion had an average of 46 tumors per mouse with an average tumor load of 3.4 mm^3. This equates to a 60% inhibition of tumor number (p<0.05) and a 74% inhibition of tumor load (p=0.05) in mice with CLPTM1L depletion. Mice with TERT depletion had an average of 122 tumors per mouse with an average tumor load of 10.2 mm^3 and were statistically similar to the control group (p=0.58). The low dose group was counted at 28 weeks post-infection. Scrambled control and shTERT mice had an average of 6 and 5 tumors, with average tumor loads of 0.50 and 0.41 mm^3 respectively (Figure 7D and 7E). Only one mouse with CLPTM1L shRNA (n=7) had a single tumor for an average tumor number of 0.14 and load of 0.01 mm^3. This represents 98% inhibition of both tumor number and load (p<0.005 and p<0.005 respectively). There was no significant difference or trend in tumor number or load between scrambled shRNA mice and mice with TERT depletion.

Discussion

The association of high CLPTM1L expression with disease SNPs at the 5p locus is highly suggestive that cis-regulation of CLPTM1L expression contributes to lung cancer risk. It is expression in normal lung tissue, rather than in tumor tissue that is relevant to cancer susceptibility. Therefore our SNP association analysis focused on normal tissue. The majority of tumors may acquire increased CLPTM1L expression regardless of genotype or the effect of genotype on basal expression. In accordance with this notion, the correlation of genotype with expression in tumor tissues trended higher with the risk genotype but was not significant (data not shown). Our results agree with the study by Grundberg et al. (26), which showed cis-regulation of CLPTM1L expression in adipose tissue of 856 healthy female twins (Figure S3). This twins study was able to separate heritable expression differences from those influenced by environment. By regulatory trait concordance (RTC) methodology, the authors showed perfect concordance of CLPTM1L regulatory SNPs with lung cancer risk SNPs suggesting that cis-regulation of this gene is likely involved in heritable risk. We intend to perform eQTL studies on a larger number of normal lung tissues to thoroughly investigate the relationship of CLPTM1L cis-regulation with lung cancer risk.

Results of our *in-vivo* tumorigenesis experiments demonstrate for the first time that CLPTM1L likely plays a pro-tumorigenic role in lung cancer. Proliferative rate in Beas-2B immortalized bronchial epithelial cells was not affected by CLPTM1L depletion, demonstrating that CLPTM1L is not required for normal proliferative function (Figure S6). Although CLPTM1L was necessary for anchorage independent survival of both A549 and H838 lung tumor cells, proliferation on an adherent surface was only affected in H838 cells with CLPTM1L loss in association with increased cell death, not in A549 cells. However, A549 cell xenograft tumorigenesis was robustly and significantly inhibited upon depletion of CLPTM1L. This is presumably due to the demonstrated dependence on CLPTM1L for

anchorage independent survival. The effect of CLPTM1L depletion on Ras driven lung tumorigenesis was quite striking; significantly inhibiting both tumor incidence and load by up to 98%. This approach to validate modifiers of tumorigenesis allows for the inhibition of expression of a gene of interest with shRNA concurrently and exclusively in cells that are K-Ras^{G12D} induced (25). Our study further demonstrates the utility of this model to validate modifiers of lung tumorigenesis, without necessitating the need to generate and/or cross the corresponding knockouts. This is especially useful in the investigation of candidate genes identified by lung cancer GWAS.

We did not see an effect on tumorigenesis with knockdown of TERT expression. This may indicate one or a combination of the following; 1) TERT expression does not immediately and directly affect lung tumorigenesis, 2) this model may miss indirect, long-term or trans-generational affects, potentially related to maintenance of telomere length, 3) longer telomere length in the mouse may mask the effect of TERT knockdown, and 4) inefficient knockdown of TERT *in-vivo*. Mice with shTERT also served as an additional non-specific control for CLPTM1L knockdown mice. TERT is well studied for its role in telomere maintenance, bypass of replicative senescence and cellular immortalization. It is commonly overexpressed in tumor tissue (reviewed in (28)). Overexpression of TERT allows cellular immortalization through telomere maintenance, which is the most likely mechanism by which TERT may contribute to the 5p association with cancer risk. A recent study suggests that 5p risk variants may be associated with hyper-methylation in the TERT promoter (29), however existing data regarding association of 5p variants with TERT expression and telomere maintenance is conflicting at best (30–32). In an analysis of SNPs in the 5p region, we have found that lung cancer associated SNPs are not associated with telomere length (Figure S7), which is in agreement with two other studies (33, 34). In contrast, a study by Rafnar et al. showed an association between 5p variants (rs401681 and rs2736098) and telomere length (p=0.017 and 0.027, respectively), although this effect was only seen in women older than 75 years with homozygous genotypes (35).

Our demonstration that stable depletion of CLPTM1L ablates morphologic transformation and anchorage independent growth of NIH3T3 cells by oncogenic H-Ras or K-Ras establishes CLPTM1L as possessing an important pro-tumorigenic function relevant to not only cancer of the lung, but other cancers as well. We did not compare inhibition of colony formation by CLPTM1L depletion between Ras isoforms since equal numbers of cells were not used in K-Ras and H-Ras experiments. Given some heterogeneity in knockdown in a pooled population of cells and in the assay system, 100% inhibition would not be expected. The results obtained were quite robust for assays of this type. It is known that H-Ras and K-Ras can prevent down-regulation of Bcl-xL upon detachment from the extracellular matrix, thereby avoiding anoikis, or apoptosis due to detachment (36). Here we present evidence that CLPTM1L is necessary for the sustained Ras induced accumulation of Bcl-xL. Depletion of CLPTM1L and the resultant depletion of survival signals are associated with a nearly complete reversion of spheroid formation and anchorage independent growth induced by Ras. Interestingly, depletion of CLPTM1L ablated Ras induced AKT phosphorylation. The addiction of cancers to Ras can be reduced to PI3K/AKT signaling (37). NFκB signaling, which is downstream of AKT, has recently been shown to be required for lung tumorigenesis in a K-Ras driven model very similar to that used in this study (38), although

we did not see strong evidence that NFκB dependent transcription was significantly affected by CLPTM1L (data not shown). AKT signaling is known to confer resistance to anoikis (39–41) and apoptosis induced by TRAIL (39), etoposide chemotherapy (42)and the p53 pathway (42, 43). Together, these data suggest that CLPTM1L may be an important regulator of the AKT survival signaling pathway. In fact, constitutively active AKT restores the transforming phenotype of Ras in CLPTM1L depleted cells. The interaction of CLPTM1L with PI3K is likely to be necessary for its function, providing a potential target for therapy if the nature of the interaction is delineated. Investigation of this interaction and how it may be targeted will be the subject of future studies. However, Bcl-xL expression, modulation of which is required for the effect of CLPTM1L on genotoxic apoptosis in human lung tumor cells (2), was unaffected by constitutively active AKT, suggesting that CLPTM1L may promote survival of tumor cells by mechanisms in addition to AKT signaling. The effect of CLPTM1L appears to be upstream of both AKT signaling and Bcl-xL stabilization, both of which may independently play a role in the pro-tumorigenic effect of CLPTM1L. Abrogation of the effect of CLPTM1L depletion on K-Ras transformation by either myrAKT or Bcl-xL expression mechanistically implicates these pathways in CLPTM1L dependent oncogenic transformation. The fact that both AKT signaling and Bcl-xL expression must be concomitantly inhibited to reverse Ras transformation is of great clinical importance. It has recently been shown that inhibition of Bcl-xL inhibition is synergistic with PI3K/AKT inhibition in human cancer (44).

Since the effect of CLPTM1L is apparently through regulation of mitochondrial apoptosis, and since the CLPTM1L locus is associated with all lung cancer histologies (21), we hypothesize that its effect may not be exclusive to Ras mutant driven tumors, but may rather influence any tumors with aberrant growth signaling. In agreement with this premise, a majority of lung tumors we tested over-expressed CLPTM1L compared to adjacent normal tissue, a much higher number than would be expected to harbor K-Ras mutations. DNA was unavailable for mutational analysis in these patients and all available RNA was utilized. In support of the hypothesis that the effect of CLPTM1L is not exclusive to Ras driven tumors, we did not observe higher CLPTM1L expression in lung tumor cell lines harboring oncogenic K-Ras mutations than those with wild type K-Ras (data not shown). Nevertheless, conclusive determination of CLPTM1L levels in relation to K-Ras mutation is warranted. Likewise, investigation of the effect of CLPTM1L on transformation by mutant forms of other common oncogenes such as EGFR is justified.

It has been shown that depletion of Bcl-xL with siRNA can sensitize cisplatin resistant human lung adenocarcinoma cells (45). Our previous studies have shown that Bcl-xL, but not other apoptotic regulators Bcl-2 and Bax, is regulated by CLPTM1L and that this regulation is required for the effect on cisplatin sensitivity (2). Similar in-vitro results in regard to regulation of survival proteins and resistance to apoptosis were obtained in Spon8 mouse lung tumor cells (Figure S4) and in H838 human lung tumor cells (2), which are p53 mutant (184G>T; p.E62*), suggesting that the effect is not exclusive to p53 wild type lung cancers and that the phenotype is repeatable in multiple cell lines. H838 cells are wild type for all Ras isoforms, again suggesting that the effects are not specific to Ras transformed cells. In fact, induction of anoikis upon CLPTM1L depletion was more significant in H838 cells than in A549 cells. Protection from apoptosis upon DNA damage may lead to an

accumulation of such damage and subsequent accumulation of mutations leading to cancer. In fact, the lung cancer associated SNP rs402710 within *CLPTM1L*, has recently been found to be associated with high levels of bulky aromatic and hydrophobic DNA adducts (46).

Together these results strongly implicate CLPTM1L dependent protection from apoptosis through regulation of survival signaling as a mechanism necessary for Ras transformation and lung tumorigenesis. The current study demonstrates a clear tumorigenic role for CLPTM1L, which until now has only been functionally related to cisplatin resistance in ovarian tumor cells (1). High CLPTM1L expression may represent an important biomarker for chemoresistance and tumor progression, and there is high potential for its use as a therapeutic target influencing anoikis and anchorage independent growth. These findings justify further investigation of the influence of CLPTM1L on cancer risk, its function and its use as a target for cancer prevention, treatment and sensitization to genotoxic therapy.

Supplementary Material

Refer to Web version on PubMed Central for supplementary material.

Acknowledgments

References

1. Yamamoto K, Okamoto A, Isonishi S, Ochiai K, Ohtake Y. A novel gene, CRR9, which was up-regulated in CDDP-resistant ovarian tumor cell line, was associated with apoptosis. Biochem Biophys Res Commun. 2001; 280:1148–54. [PubMed: 11162647]

2. James M, WW, YW, LAB, JVH, KRC, et al. Functional characterization of CLPTM1L as a lung cancer risk candidate gene in the 5p15.33 locus. PLoS One. 2012; 7:e36116. [PubMed: 22675468]

3. Ni Z, Tao K, Chen G, Chen Q, Tang J, Luo X, et al. CLPTM1L Is Overexpressed in Lung Cancer and Associated with Apoptosis. PLoS One. 2012; 7:e52598. [PubMed: 23300716]

4. Grad JM, Zeng X-R, Boise LH. Regulation of Bcl-xL: a little bit of this and a little bit of STAT. Current Opinion in Oncology. 2000; 12:543–9. [PubMed: 11085453]

5. Behrends C, Sowa ME, Gygi SP, Harper JW. Network organization of the human autophagy system. Nature. 2010; 466:68–76. [PubMed: 20562859]

6. Carnero A. The PKB/AKT pathway in cancer. Curr Pharm Des. 2010; 16:34–44. [PubMed: 20214616]

7. Chen C, Edelstein LC, Gelinas C. The Rel/NF-kappaB family directly activates expression of the apoptosis inhibitor Bcl-x(L). Mol Cell Biol. 2000; 20:2687–95. [PubMed: 10733571]

8. Chen XF, Cai S, Chen QG, Ni ZH, Tang JH, Xu DW, et al. Multiple variants of TERT and CLPTM1L constitute risk factors for lung adenocarcinoma. Genet Mol Res. 2012; 11:370–8. [PubMed: 22370939]

9. Pande M, Spitz MR, Wu X, Gorlov IP, Chen WV, Amos CI. Novel genetic variants in the chromosome 5p15.33 region associate with lung cancer risk. Carcinogenesis. 2011; 32:1493–9. [PubMed: 21771723]

10. Wang S, Wu J, Hu L, Ding C, Kan Y, Shen Y, et al. Common genetic variants in TERT contribute to risk of cervical cancer in a Chinese population. Mol Carcinog. 2012

11. McKay JD, Hung RJ, Gaborieau V, Boffetta P, Chabrier A, Byrnes G, et al. Lung cancer susceptibility locus at 5p15.33. Nat Genet. 2008; 40:1404–6. [PubMed: 18978790]

12. Wang Y, Broderick P, Webb E, Wu X, Vijayakrishnan J, Matakidou A, et al. Common 5p15.33 and 6p21.33 variants influence lung cancer risk. Nat Genet. 2008; 40:1407–9. [PubMed: 18978787]

13. Petersen GM, Amundadottir L, Fuchs CS, Kraft P, Stolzenberg-Solomon RZ, Jacobs KB, et al. A genome-wide association study identifies pancreatic cancer susceptibility loci on chromosomes 13q22.1, 1q32.1 and 5p15.33. Nat Genet. 2010; 42:224–8. [PubMed: 20101243]

14. Rothman N, Garcia-Closas M, Chatterjee N, Malats N, Wu X, Figueroa JD, et al. A multi-stage genome-wide association study of bladder cancer identifies multiple susceptibility loci. Nat Genet. 2010; 42:978–84. [PubMed: 20972438]

15. Landi MT, Chatterjee N, Yu K, Goldin LR, Goldstein AM, Rotunno M, et al. A Genome-wide Association Study of Lung Cancer Identifies a Region of Chromosome 5p15 Associated with Risk for Adenocarcinoma. The American Journal of Human Genetics. 2009; 85:679–91. [PubMed: 19836008]

16. Zhao Y, Chen G, Song X, Chen H, Mao Y, Lu D. Fine-mapping of a region of chromosome 5p15.33 (TERT-CLPTM1L) suggests a novel locus in TERT and a CLPTM1L haplotype are associated with glioma susceptibility in a Chinese population. Int J Cancer. 2011

17. Liu P, Vikis HG, Lu Y, Wang Y, Schwartz AG, Pinney SM, et al. Cumulative effect of multiple loci on genetic susceptibility to familial lung cancer. Cancer Epidemiol Biomarkers Prev. 2010; 19:517–24. [PubMed: 20142248]

18. Yin J, Li Y, Yin M, Sun J, Liu L, Qin Q, et al. *TERT-CLPTM1L* Polymorphism rs401681 Contributes to Cancers Risk: Evidence from a Meta-Analysis Based on 29 Publications. PLoS One. 2012; 7:e50650. [PubMed: 23226346]

19. Vazquez-Mena O, Medina-Martinez I, Juarez-Torres E, Barron V, Espinosa A, Villegas-Sepulveda N, et al. Amplified genes may be overexpressed, unchanged, or downregulated in cervical cancer cell lines. PLoS One. 2012; 7:e32667. [PubMed: 22412903]

20. Kang JU, Koo SH, Kwon KC, Park JW, Kim JM. Gain at chromosomal region 5p15.33, containing TERT, is the most frequent genetic event in early stages of non-small cell lung cancer. Cancer Genet Cytogenet. 2008; 182:1–11. [PubMed: 18328944]

21. Timofeeva MN, Hung RJ, Rafnar T, Christiani DC, Field JK, Bickeböller H, et al. Influence of common genetic variation on lung cancer risk: meta-analysis of 14 900 cases and 29 485 controls. Human Molecular Genetics. 2012

22. McDoniels-Silvers AL, Herzog CR, Tyson FL, Malkinson AM, You M. Inactivation of both Rb and p53 pathways in mouse lung epithelial cell lines. Exp Lung Res. 2001; 27:297–318. [PubMed: 11293330]

23. Herzog CR, Soloff EV, McDoniels AL, Tyson FL, Malkinson AM, Haugen-Strano A, et al. Homozygous codeletion and differential decreased expression of p15INK4b, p16INK4a-alpha and p16INK4a-beta in mouse lung tumor cells. Oncogene. 1996; 13:1885–91. [PubMed: 8934534]

24. Schneider CA, Rasband WS, Eliceiri KW. NIH Image to ImageJ: 25 years of image analysis. Nature Methods. 2012; 9:671–5. [PubMed: 22930834]

25. DuPage M, Dooley AL, Jacks T. Conditional mouse lung cancer models using adenoviral or lentiviral delivery of Cre recombinase. Nat Protoc. 2009; 4:1064–72. [PubMed: 19561589]

26. Grundberg E, Small KS, Hedman AK, Nica AC, Buil A, Keildson S, et al. Mapping cis- and trans-regulatory effects across multiple tissues in twins. Nat Genet. 2012 advance online publication.

27. Guerrero S, Casanova I, Farre L, Mazo A, Capella G, Mangues R. K-ras codon 12 mutation induces higher level of resistance to apoptosis and predisposition to anchorage-independent growth than codon 13 mutation or proto-oncogene overexpression. Cancer Res. 2000; 60:6750–6. [PubMed: 11118062]

28. Chen CH, Chen RJ. Prevalence of telomerase activity in human cancer. J Formos Med Assoc. 2011; 110:275–89. [PubMed: 21621148]

29. Scherf DB, Sarkisyan N, Jacobsson H, Claus R, Bermejo JL, Peil B, et al. Epigenetic screen identifies genotype-specific promoter DNA methylation and oncogenic potential of CHRNB4. Oncogene. 2012

30. Mirabello L, Yu K, Kraft P, De Vivo I, Hunter DJ, Prescott J, et al. The association of telomere length and genetic variation in telomere biology genes. Hum Mutat. 2010

31. Pooley KA, Tyrer J, Shah M, Driver KE, Leyland J, Brown J, et al. No Association between TERT-CLPTM1L Single Nucleotide Polymorphism rs401681 and Mean Telomere Length or Cancer Risk. Cancer Epidemiol Biomarkers Prev. 2010

32. Fehringer G, Liu G, Pintilie M, Sykes J, Cheng D, Liu N, et al. Association of the 15q25 and 5p15 lung cancer susceptibility regions with gene expression in lung tumour tissue. Cancer Epidemiol Biomarkers Prev. 2012

33. Pooley KA, Tyrer J, Shah M, Driver KE, Leyland J, Brown J, et al. No Association between TERT-CLPTM1L Single Nucleotide Polymorphism rs401681 and Mean Telomere Length or Cancer Risk. Cancer Epidemiol Biomarkers Prev.

34. Mirabello L, Yu K, Kraft P, De Vivo I, Hunter DJ, Prescott J, et al. The association of telomere length and genetic variation in telomere biology genes. Hum Mutat.

35. Rafnar T, Sulem P, Stacey SN, Geller F, Gudmundsson J, Sigurdsson A, et al. Sequence variants at the TERT-CLPTM1L locus associate with many cancer types. Nat Genet. 2009; 41:221–7. [PubMed: 19151717]

36. Rosen K, Rak J, Leung T, Dean NM, Kerbel RS, Filmus J. Activated Ras prevents downregulation of Bcl-X(L) triggered by detachment from the extracellular matrix. A mechanism of Ras-induced resistance to anoikis in intestinal epithelial cells. J Cell Biol. 2000; 149:447–56. [PubMed: 10769035]

37. Lim KH, Counter CM. Reduction in the requirement of oncogenic Ras signaling to activation of PI3K/AKT pathway during tumor maintenance. Cancer Cell. 2005; 8:381–92. [PubMed: 16286246]

38. Meylan E, Dooley AL, Feldser DM, Shen L, Turk E, Ouyang C, et al. Requirement for NF-kappaB signalling in a mouse model of lung adenocarcinoma. Nature. 2009; 462:104–7. [PubMed: 19847165]

39. Koci L, Hyzd'alova M, Vaculova A, Hofmanova J, Kozubik A. Detachment-mediated resistance to TRAIL-induced apoptosis is associated with stimulation of the PI3K/Akt pathway in fetal and adenocarcinoma epithelial colon cells. Cytokine. 2011; 55:34–9. [PubMed: 21482133]

40. Liu SG, Wang BS, Jiang YY, Zhang TT, Shi ZZ, Yang Y, et al. Atypical protein kinase Ciota (PKCiota) promotes metastasis of esophageal squamous cell carcinoma by enhancing resistance to Anoikis via PKCiota-SKP2-AKT pathway. Mol Cancer Res. 2011; 9:390–402. [PubMed: 21310827]

41. Du XL, Yang H, Liu SG, Luo ML, Hao JJ, Zhang Y, et al. Calreticulin promotes cell motility and enhances resistance to anoikis through STAT3-CTTN-Akt pathway in esophageal squamous cell carcinoma. Oncogene. 2009; 28:3714–22. [PubMed: 19684620]

42. Mayo LD, Dixon JE, Durden DL, Tonks NK, Donner DB. PTEN protects p53 from Mdm2 and sensitizes cancer cells to chemotherapy. J Biol Chem. 2002; 277:5484–9. [PubMed: 11729185]

43. Mayo LD, Donner DB. The PTEN, Mdm2, p53 tumor suppressor-oncoprotein network. Trends Biochem Sci. 2002; 27:462–7. [PubMed: 12217521]

44. Rahmani M, Aust MM, Attkisson E, Williams DC Jr, Ferreira-Gonzalez A, Grant S. Dual inhibition of Bcl-2 and Bcl-xL strikingly enhances PI3K inhibition-induced apoptosis in human myeloid leukemia cells through a GSK3- and Bim-dependent mechanism. Cancer Res. 2012

45. Lei X, Huang Z, Zhong M, Zhu B, Tang S, Liao D. Bcl-XL small interfering RNA sensitizes cisplatin-resistant human lung adenocarcinoma cells. Acta Biochim Biophys Sin (Shanghai). 2007; 39:344–50. [PubMed: 17492131]

46. Zienolddiny S, Skaug V, Landvik NE, Ryberg D, Phillips DH, Houlston R, et al. The TERT-CLPTM1L lung cancer susceptibility variant associates with higher DNA adduct formation in the lung. Carcinogenesis. 2009; 30:1368–71. [PubMed: 19465454]

47. McDoniels-Silvers AL, Herzog CR, Tyson FL, Malkinson AM, You M. Inactivation of both Rb and p53 pathways in mouse lung epithelial cell lines. Exp Lung Res. 2001; 27:297–318. [PubMed: 11293330]

48. Welcome Trust, Sanger Institute. Multiple Tissue Human Expression Resource. 2013. Available from: http://www.muther.ac.uk/

49. Welcome Trust, Sanger Institute. Genevar. Available from: http://www.sanger.ac.uk/resources/software/genevar/

A

B
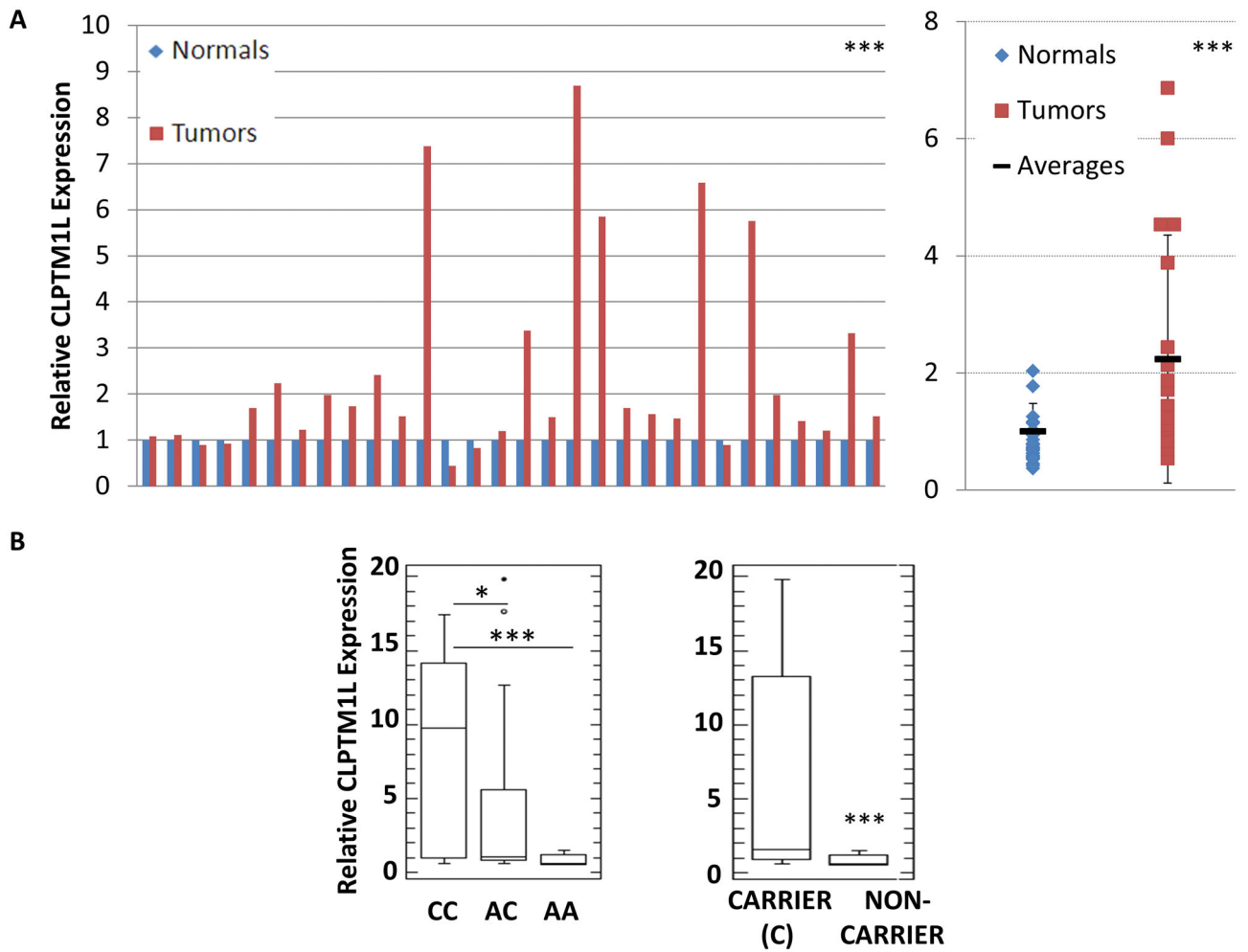
Figure 1. CLPTM1L is Overexpressed in Lung Adenocarcinomas and is Regulated in Normal Lung Tissue by Lung Cancer Risk Variants

A) Left Panel: CLPTM1L transcript accumulation in human lung adenocarcinoma tissue, expressed as relative to each paired normal adjacent tissue. P-value obtained by paired Student's *t*-Test. Right Panel: CLPTM1L transcript accumulation in human lung adenocarcinomas and adjacent normal lung tissues, expressed as relative to the average value for normal tissues. Error bars represent one SD from the mean. B) Box plots of eQTL analysis of the association of expression of CLPTM1L transcript in normal lung tissues as measured by RT-qPCR and genotype of the lung cancer associated SNP rs31489. X axis labels represent the genotype of the rs31489 SNP. Center line is the median, boxes represent the 1st and 3rd quartiles, whiskers represent 10th to 90th percentile, open dots represent suspected outliers within 1 inter-quartile range of the whiskers and closed dots represent outliers outside 1 inter-quartile ranges outside the whiskers. * $p < 0.05$, ** $p < 0.005$, *** $p < 0.0005$
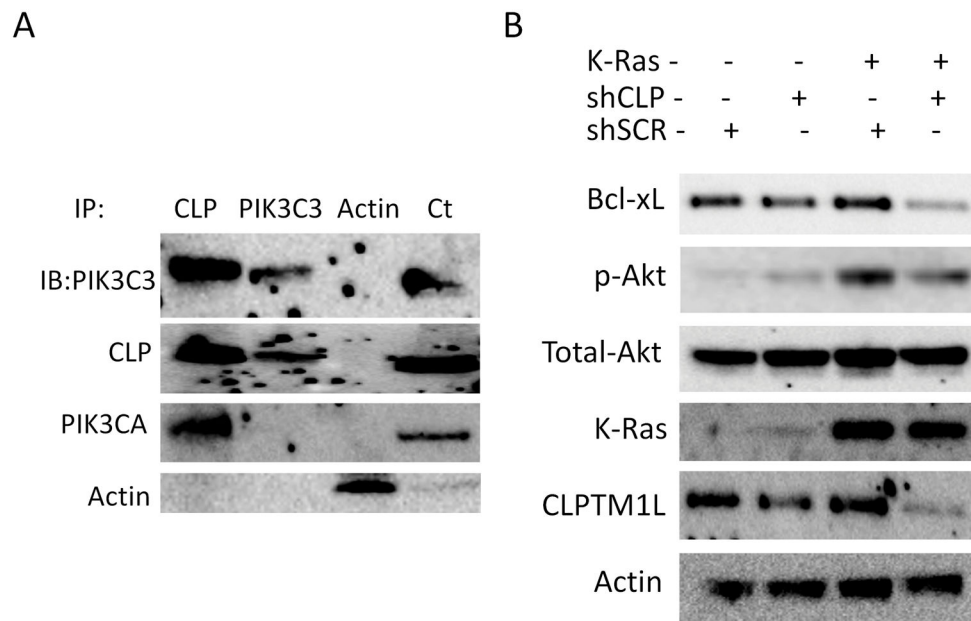
Figure 2. CLPTM1L Regulates AKT Pathway and Bcl-xL Accumulation
A) Co-Immunoprecipitation of PIK3C3, PIK3CA and CLPTM1L from NIH3T3 cell lysates using each as bait or prey. Actin represents a non-specific control IP antibody. The control column represents lysate passed through an Actin antibody loaded column (lysate with no relevant immunoprecipitation). B) Representative western blots for phosphorylated and total AKT, Bcl-xL, K-Ras and CLPTM1L in NIH3T3 cells with KRas^{V12} expression and/or shRNA CLPTM1L depletion or scrambled shRNA control.
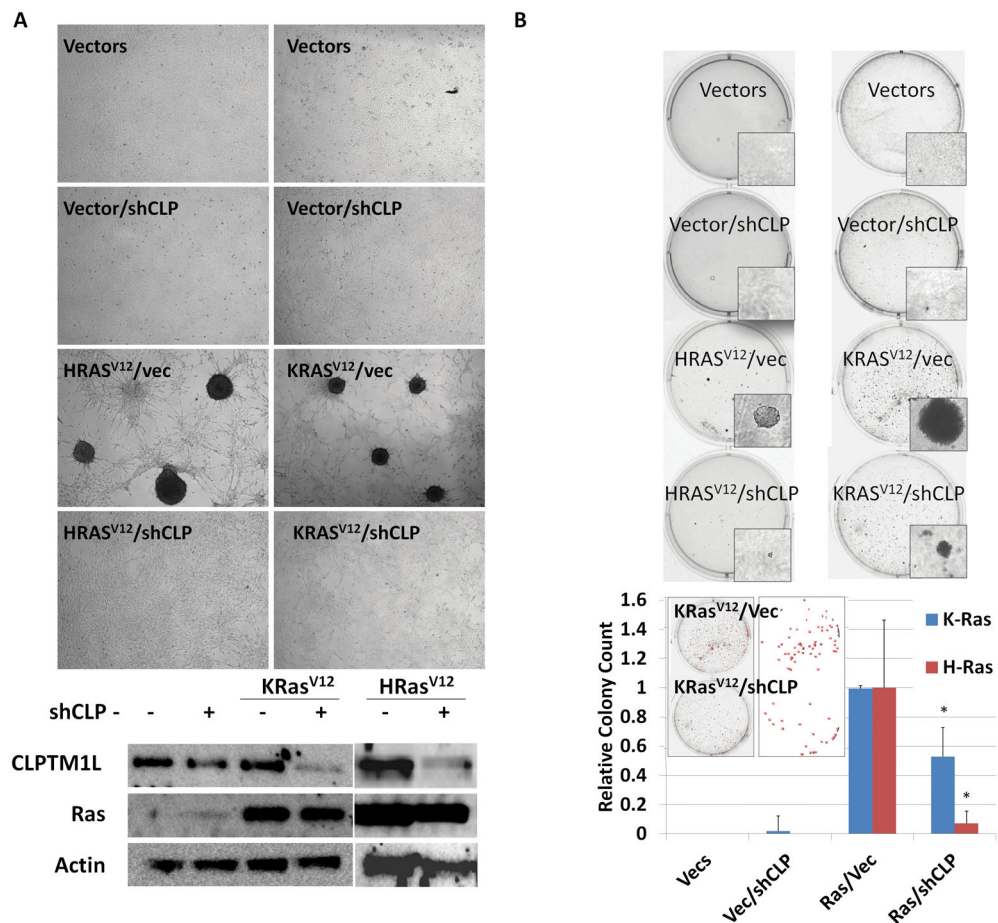
Figure 3. CLPTM1L is Required for Ras Oncogenic Transformation of Mouse Fibroblasts
A) Micrographs of NIH3T3 cells stably transfected with oncogenic Ras isoforms or vector controls as well as shRNA CLPTM1L depletion or scrambled shRNA control. Representative western blots for CLPTM1L depletion and Ras expression (below). B) Representative wells of soft agar anchorage independent growth assays in of NIH3T3 cells stably transfected with oncogenic Ras isoforms or vector controls as well as shRNA CLPTM1L depletion or scrambled shRNA control vector. Bottom panel: graphic representation of relative anchorage independent colony numbers as counted using Image J software. P-values obtained by two tailed Student's *t*-Test. * p<0.05
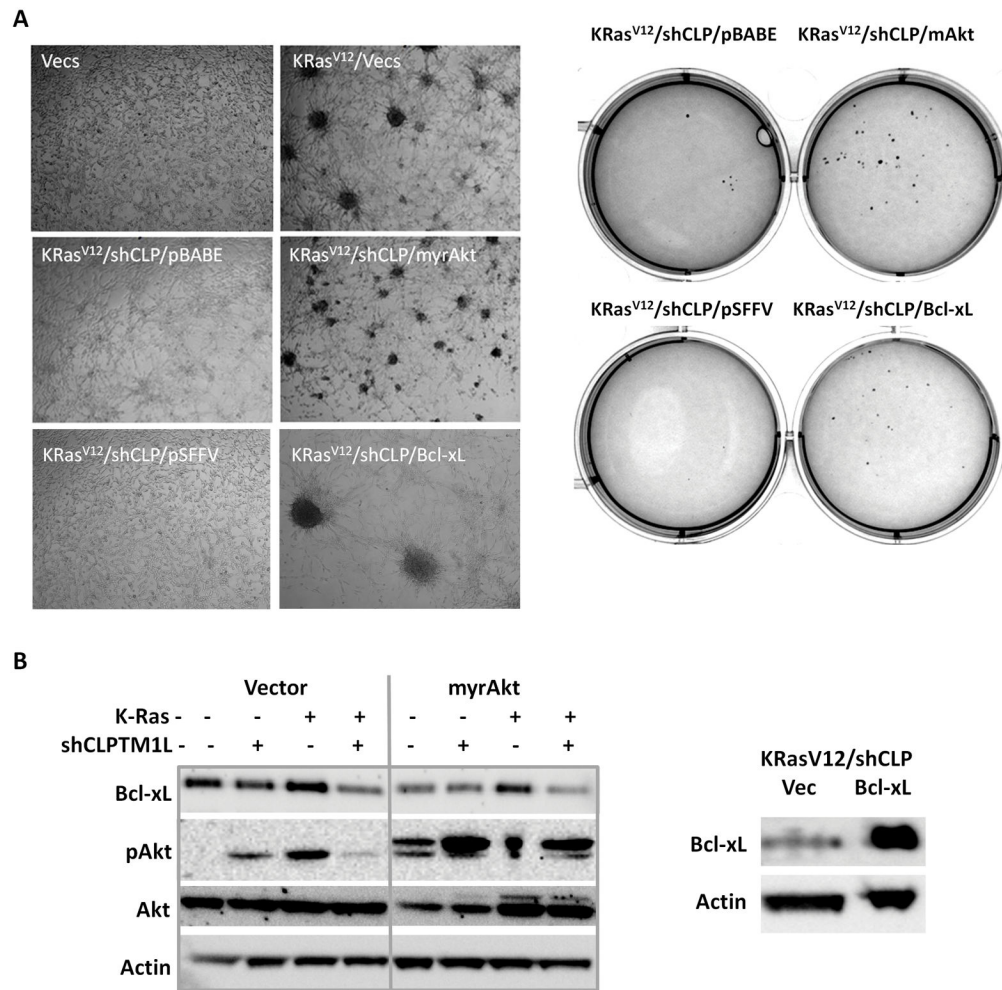
Figure 4. Either AKT Phosphorylation or Bcl-xL Expression is Sufficient for CLPTM1L Dependent Ras Oncogenic Transformation

A) Micrographs of NIH3T3 cells stably transfected with KRas^{V12} and shRNA CLPTM1L depletion or scrambled shRNA control as in previous figures transfected with either constitutively active myrAKT, Bcl-xL or vector controls. Visible colonies in representative wells (right). B) Western blotting for apoptotic regulators in NIH3T3 cells with and without myrAKT expression as described in Fig. 5A. C) Western blotting for exogenous Bcl-xL re-expression. * p<0.05
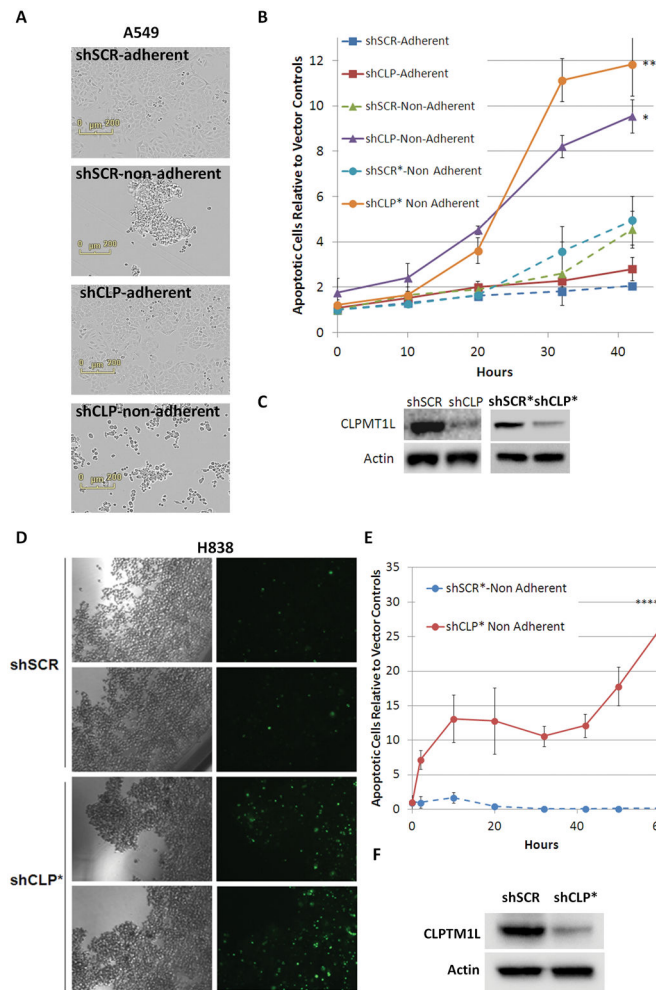
Figure 5. CLPTM1L is Required for Survival Upon Detachment of Human Lung Tumor Cells
A) Representative micrographs of A549 cells cultured on poly-HEMA coated non-adherent plates or conventional treated plates. B) Anoikis assay (real-time quantification of caspase 3 positivity in live cells) on A549 cells with CLPTM1L depletion with two shRNA vectors, shCLP and shCLP* or scrambled shRNA control grown on either a conventional or non-adherent surface. Squares-shCLP and control on adherent surface, Triangles-shCLP and control on non-adherent surface, Circles-second construct shCLP* and corresponding control. Vector controls are represented with dotted lines. P-values obtained by two tailed Student's *t*-Test. *p<0.05, ***p<0.0005 C) Western blotting for CLPTM1L in A549 with each shRNA CLPTM1L depletion or vector control. D) H838 cells grown on non-adherent poly-HEMA coated plates with Caspase 3/7 activity as indicated by green fluorescence after 64 hours (Right panels). E) Apoptotic cells per well relative to starting vector control values inH838 with scrambled control or shCLP* as measured in a live cell imager. Twelve replicates per group. Bars= one standard error of the mean. ****p<5×10^{-6} F) Western blotting confirming CLPTM1L depletion.
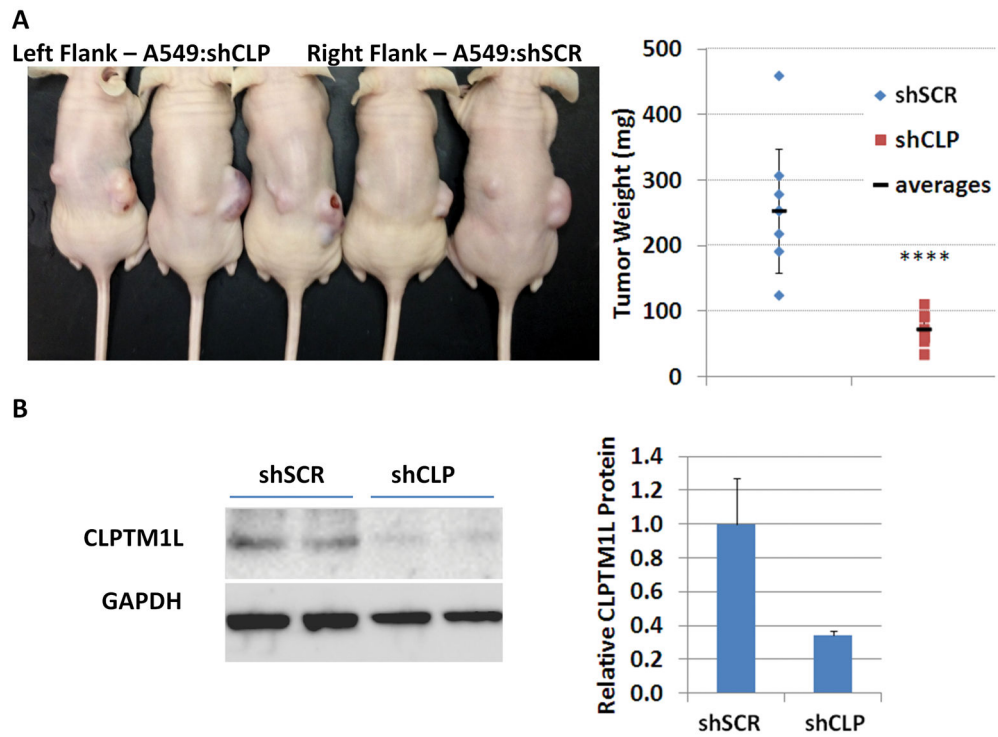
Figure 6. CLPTM1L is Required for Tumorigenesis in a Human Lung Tumor Xenograft Model
A) Athymic nude mouse xenograft tumorigenesis assays with 5×10^5 A549 stably transduced with shCLP (left flank) or 5×10^5 A549 stably transduced with scrambled shRNA control (right flank) four weeks after implantation of tumor cells. Tumor weights four weeks after implantation of tumor cells. ****- $p < 0.00005$ B) Western blotting for CLPTM1L protein accumulation in tumor tissue. Quantification GAPDH normalized relative CLPTM1L accumulation using Image J software.
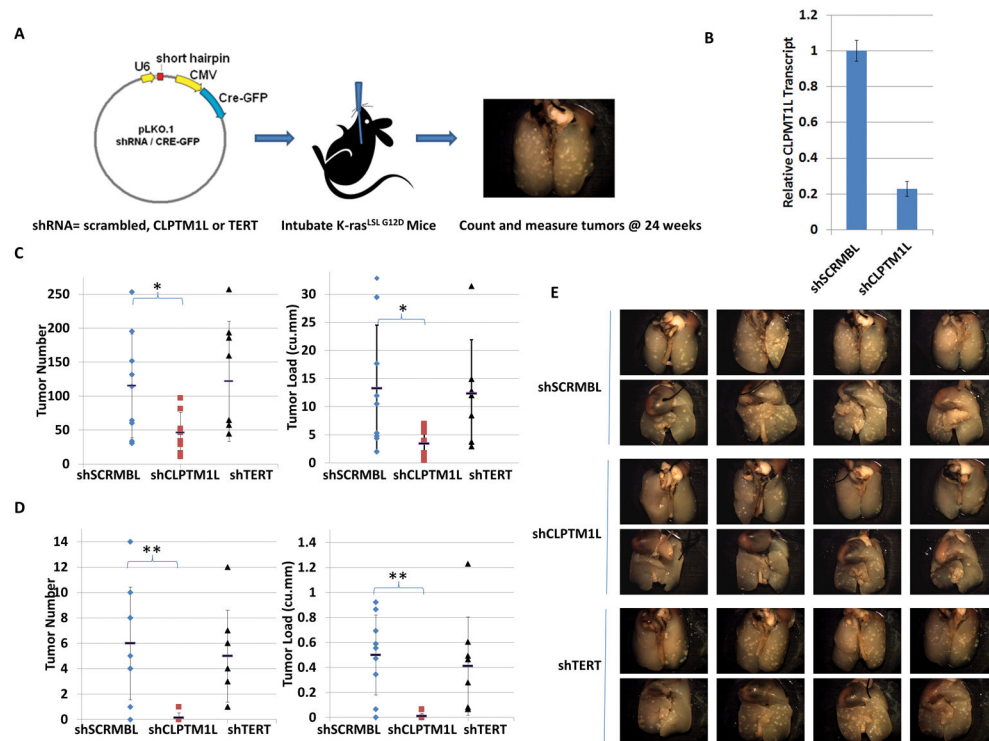
Figure 7. CLPTM1L is Required for KRas Driven Lung Tumorigenesis
A) Diagram of K-Ras$^{+/LSLG12D}$ mouse model of lung tumorigenesis allowing concurrent modulation of candidate gene expression. B) Relative CLPTM1L transcript accumulation in mouse tumor cells with shSCRMBL vector or shCLPTM1L as measured by quantitative real-time PCR. C) High dose group: Tumor number (left panel) and tumor load (right panel) for mice infected with virus encoding shRNA for random scrambled sequence, CLPTM1L and TERT. Black bars represent the mean. Error bars represent one standard deviation from the mean. D) Low dose group: as in Figure 7C. E) Representative gross appearance of lungs from scrambled shRNA, CLPTM1L shRNA and TERT shRNA high dose groups. * p<0.05, ** p<0.005